

# Estimating Local Part Thickness in Midplane Meshes for Finite Element Analysis

Vânio Ferreira, Luís Paulo Santos, Markus Franzen, Omar O. Ghouati, Ricardo Simões

**Abstract**—Within the development of motor vehicles, crash safety (e.g. occupant protection, pedestrian protection, low speed damageability), is one of the most important attributes. In order to be able to fulfill the increased requirements in the framework of shorter cycle times and rising pressure to reduce costs, car manufacturers keep intensifying the use of virtual development tools such as those in the domain of Computer Aided Engineering (CAE). For crash simulations, the explicit finite element method (FEM) is applied. The accuracy of the simulation process is highly dependent on the accuracy of the simulation model, including the midplane mesh. One of the roughest approximations typically made is the actual part thickness which, in reality, can vary locally. However, almost always a constant thickness value is defined throughout the entire part due to complexity reasons. On the other hand, for precise fracture analysis within FEM, the correct thickness consideration is one key enabler.

Thus, availability of per element thickness information, which does not exist explicitly in the FEM model, can significantly contribute to an improved crash simulation quality, especially regarding fracture prediction. Even though the thickness is not explicitly available from the FEM model, it can be inferred from the original CAD geometric model through geometric calculations. This paper proposes and compares two thickness estimation algorithms based on ray tracing and nearest neighbour 3D range searches. A systematic quantitative analysis of the accuracy of both algorithms is presented, as well as a thorough identification of particular geometric arrangements under which their accuracy can be compared. These results enable the identification of each technique's weaknesses and hint towards a new, integrated, approach to the problem that linearly combines the estimates produced by each algorithm.

**Index Terms**—Automotive crash simulations, structural modelling, FEM mesh, thickness estimation, ray tracing

## I. INTRODUCTION

Today, the automotive industry is challenged with a continuous rising number of demands taking a strong influence on the development process. The need for CO<sub>2</sub> reduction and hence the resulting need to reduce the vehicle weight as well as the need to constantly improve occupant and pedestrian protection makes it necessary to fully utilize the deployed materials as efficiently as possible. In addition, product development has to be economical with respect to development time and costs. For crash simulations the explicit Finite Element Method (FEM) has been applied for a long time. However, this process can only be successful if the numerical methods are capable and have a high confidence level.

CCTC, Universidade do Minho, vaniomiguel@gmail.com and psantos@di.uminho.pt

Ford Research, Advanced Engineering Europe, [mfranzen6,oghouti]@ford.com

IPC/I3N - Universidade do Minho and Polytechnic Institute of Cávado and Ave, rsimoes@dep.uminho.pt

The properties of parts made of plastic materials are particularly difficult to predict due to the intrinsic complex behaviour of those materials. However, as plastics are pervasive in many different automotive applications, including those with very demanding specifications, it becomes vital to find adequate methods for modelling and simulating those parts under service conditions. Within the area of crash simulation of thermoplastic parts, the actual local thicknesses play a significant role for accurate deformation and fracture behaviour prediction. Due to the fact that most thermoplastic parts used in vehicles are injection moulded, the actual thickness can vary significantly throughout a part. That thickness distribution is not explicitly available within 2D crash meshes, which are those mainly used in full car crash simulations, but it exists implicitly in the full part geometry in CAD files (like IGES). However, currently there are no automated and precise ways to extract that local thickness distribution from the CAD files, seriously limiting the precision – and thus, the potential benefit – of crash simulations.

The main method currently employed for vehicle crash simulation of thermoplastic parts is the Finite Element Method (FEM). FEM is a numerical approach for calculating approximate solutions of partial differential equations and integral equations, enabling the numerical solution of many complex problems in structural mechanics, and is the standard approach for complex systems, particularly in the industry setting [1]. The main alternative methods to FEM are the Finite Differences Method and Finite Volume Method, the latter frequently applied to fluid dynamic problems [2], such as strain on structural elements with internal fluid pressure [3] or oscillator storage tanks under hydrodynamic loads [4].

In the case of FEM, the entire geometric domain of the part/system under study is discretized and modelled by a mesh (whether a midplane two-dimensional mesh, or a full three-dimensional surface or solid mesh), comprised of a large set of finite elements (which can be of several simple geometries) that intersect at points termed nodes [5], [6], [7]. Elements are then assigned properties, which can be physical (e.g. thickness, density, Young's modulus, tensile strength), thermal, electric, or others. This method was initially proposed in the 1950s for airframe and structural analysis [8]. In 1973, Strang and Fix [9] provided a rigorous mathematical foundation, and enabled its expansion to many new applications. Aside from its major application to structural mechanics, FEM has been used in a large variety of fields, including acoustics [10], fluid dynamics [11], medicine [12], and many others. FEM can also be applied for the optimization of molding tools, such as polymer injection molds [13]. The simulations can be employed to quantify the thermomechanical environment

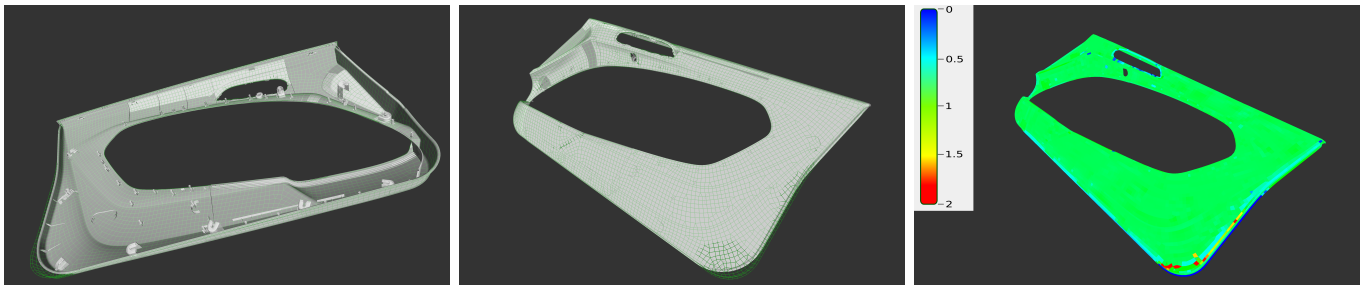


Fig. 1. Different views of a car door geometry (grey) and the respective midplane mesh (green). Ideally the midplane mesh runs inside the part's surface, but in reality it might extend outside (dark green regions). The figure at the right presents, for each element of the midplane mesh, the estimated thickness as a pseudo color map.

resulting on the mold from the injection molding process, namely the pressure and temperature distributions on the surface of the molding cavity. This combined with other information readily available from process simulations, such as optimal gate design and location, enables the optimization of the entire molding process.

Although FEM is used for these various purposes, its main application is undoubtedly the prediction of the mechanical performance of parts under load. It has enabled significant changes in product development over the past decades, both in part design, for example to select the most appropriate part thickness or even the most effective geometry for specific applications [14], and also for tools and processes, for example in determining the behavior of specific equipment components during the use of the tool/machine [15].

An aspect that should be considered when discussing FEM is concurrent engineering [16], [17], which in this context pertains to performing several simultaneous activities that are required for the analysis process, with a clear synergy between them. The most typical application of concurrent engineering in the case of polymer-based injection moulded parts is integration between structural and flow simulations [13]. This is due to the fact that the processing stage will affect the mechanical behavior of the part in service, and thus, effects resulting from the injection moulding process, such as warpage and residual stresses, should be taken into consideration for the structural simulation. Most often, different meshes are used for both types of simulation; on the one hand, due to the fact that flow simulation often employs full 3D meshes or application-related mesh types (e.g. Fusion in the Moldflow software), but on the other hand, also due to the fact that the flow simulation may include features only present in the processing stage (such as the runner system). In addition, commercial applications are usually closed and do not allow seamless transfer of meshes from one format to another, despite research efforts to that end [13]. In any case, most often the local thickness is available when performing flow simulations, but it is not considered when performing the structural simulation.

This paper proposes and compares two techniques to estimate local thicknesses from geometric models of automotive thermoplastic parts and make these estimates available to vehicle crash simulations based on finite element analysis. The geometry of the parts is described as a closed surface on a CAD file. FEM simulators use discrete approximate

representations of this geometry. These representations are meshes of polygons that, ideally, run in the middle of the closed surface – they are thus referred to as midplane meshes (see figure 1).

Creating midplane meshes is not trivial. There are many techniques and many application, both commercial and closed, for mesh generation and mesh refinement, but there is still ongoing research on finding automated (or semi-automated) procedures that enable obtaining meshes of adequate quality for simulation purposes [18], [19], [20].

Midplane meshes are generated from the CAD geometry model, but they do not contain any information about the part's local thickness. However, this information is crucial to allow accurate behaviour prediction in automotive crash simulations. The problem addressed throughout this paper is automatic estimation of thickness on a per-element basis, using as inputs the CAD geometry model and the midplane mesh itself. The proposed thickness estimation techniques, based on ray tracing and nearest neighbour 3D range searches, allow tagging each mesh element with its associated local thickness, thus empowering accurate vehicle crash simulations. The paper contribution is a systematic quantitative analysis of the accuracy of both thickness estimation techniques, as well as a thorough identification of particular geometric arrangements under which the methods' accuracy can be compromised. These results will enable identifying each technique weaknesses and suggesting new approaches to the problem. The next section presents the two thickness estimation algorithms, the methodology to use throughout this systematic assessment of their respective accuracies and an analysis of the obtained results.

Section III proposes some improvements to these algorithms that significantly increase their accuracy and the paper closes with some concluding remarks and proposals for future work.

It is important to note that all information in this paper about part thickness, including thickness calculation results, are normalized so that the real part thickness takes the value of 1. Thus, the thicknesses listed do not represent the real thickness of the case-study parts.

## II. THICKNESS ESTIMATION ALGORITHMS

Ideally, the midplane mesh runs inside the closed surface and parallel to it (see figure 2). Intuitively, in such cases the thickness at the centroid of each midplane mesh element is the

sum of the distances between this centroid and some surface point on each side of the element. With this definition in mind two thickness estimation algorithms are proposed.

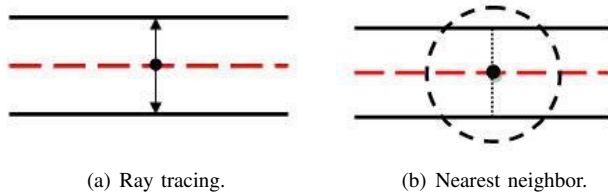


Fig. 2. Algorithms for thickness estimation. Solid black lines represent the part's geometry, the red dashed line represents the midplane mesh and the dashed circle represents the nearest neighbour search domain.

**Ray Tracing (RT)** - a ray is shot for each side of the midplane mesh element, with origin on the element's centroid and direction equal to the element's normal [21], [22]. Ideally each of these rays intersects the part's geometry; the sum of both intersections' distance is taken as an estimate of the part's local thickness.

**Nearest Neighbor (NN)** - this algorithm performs a search on the surface geometry to locate which point is nearer to the mid-plane mesh element centroid [23]. Figure 2(b) illustrates the algorithm; the dashed circle represents the search domain, which grows until the search algorithm returns a valid point on the part's surface. Actually, two such searches are performed to locate two points, each on a different side of the mid plane mesh element. The sum of the distances from the element's centroid and these two points is taken as an estimate of the part's local thickness.

Since the geometry models are themselves represented as a mesh of polygons a kd-tree is used to accelerate each of these algorithms [23]. For ray tracing the kd-tree is used for space traversal, thus reducing the total number of evaluated intersections, whereas for NN the kd-tree is used to perform a range search and locate the nearest surface point.

In the ideal case, as depicted in figure 2, both algorithms return exactly the same thickness estimate. Real parts, however, include complex geometric configurations and/or incorrect midplane mesh approximations. Correctly handling such cases requires a systematic quantitative analysis of the proposed algorithms behaviour and accuracy. Analysis of the algorithms accuracy with real automotive parts is difficult because the exact local thicknesses are unknown. In order to enable such analysis seven simple synthetic parts, whose exact thickness is known (normalized to 1 mm for all parts), were modelled and used throughout the whole validation process. For each part three different midplane meshes were supplied, corresponding to different meshing granularities. The different mesh granularities have been termed "coarse", "medium" and "fine". The "medium" mesh edge length is 2.5 times the edge length of the "fine" mesh, and the "coarse" mesh edge length is 4 times the edge length of the "fine" mesh. This allows studying the thickness estimate accuracy for different representations. Figure 3 presents these synthetic parts, which emphasize particular situations where the above described algorithms are expected to fail. Parts 1 to 4 have the midplane

mesh either total or partially outside the part's surface, parts 5 to 7 include ribs – thickness is not exactly defined at the regions where the rib intersects the main surface.

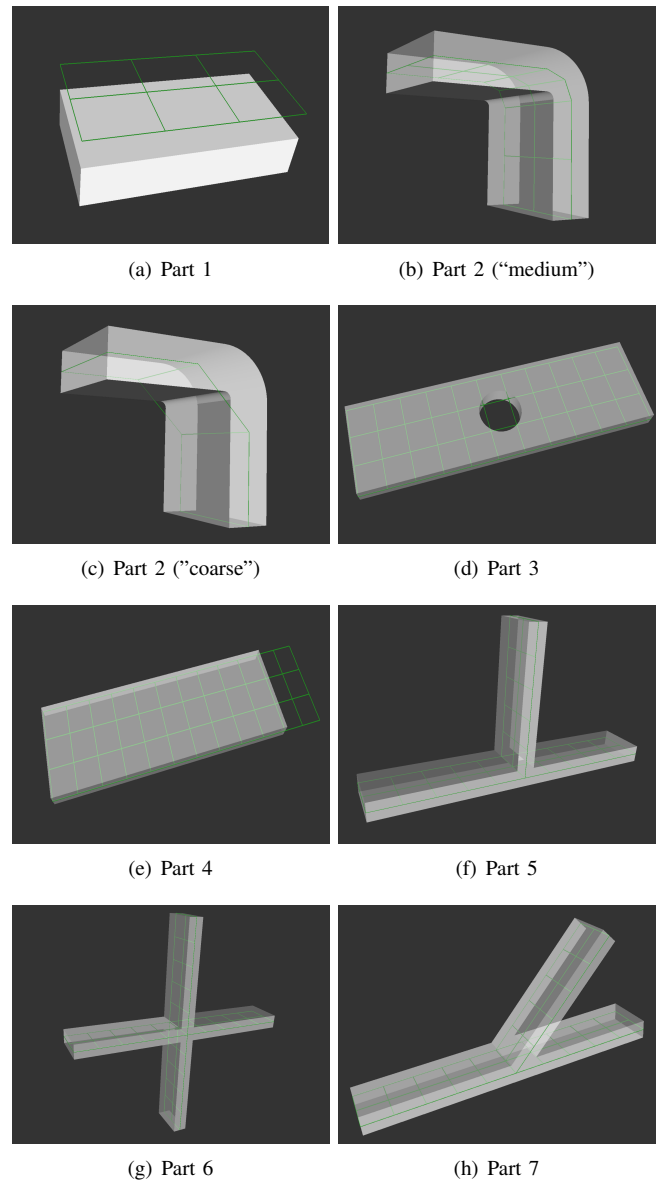


Fig. 3. Synthetic parts used for quantitative analysis of the thickness estimate accuracy.

#### A. Metrics for quantitative analysis

Knowledge of the exact thickness of the synthetic parts allows for a quantitative analysis of the thickness estimation process. This analysis requires selecting metrics that can be used as objective functions. Two such metrics are used throughout this paper: arithmetic mean and the root mean square error (RMSE). The objective function is RMSE, which must be minimized.

**Arithmetic Mean (AM)** - since the actual thickness is a constant (and equal to 1mm) across the whole surface for all the synthetic parts, the arithmetic mean  $\bar{T}$ , calculated as the average of the estimated thickness,  $\bar{T}_i$ , across all  $N$  elements

Part nbr.		Ray tracing		Nearest Neighbor	
		$\bar{T}$	RMSE	$\bar{T}$	RMSE
1	fine	0.000	1.000	0.000	1.000
	medium	0.000	1.000	0.000	1.000
	coarse	0.000	1.000	0.000	1.000
2	fine	1.000	0.001	0.883	0.169
	medium	0.999	0.001	0.999	0.001
	coarse	0.667	0.577	1.040	0.070
3	fine	0.942	0.241	0.911	0.204
	medium	0.969	0.174	1.029	0.294
	coarse	1.000	0.000	0.874	0.333
4	fine	0.857	0.378	1.194	0.865
	medium	0.833	0.408	1.287	0.883
	coarse	0.857	0.378	1.246	0.651
5	fine	1.833	3.062	0.895	0.162
	medium	1.000	0.000	0.999	0.000
	coarse	1.000	0.000	0.999	0.000
6	fine	2.250	4.330	0.912	0.141
	medium	1.000	0.000	1.000	0.000
	coarse	1.000	0.000	1.000	0.000
7	fine	1.097	0.312	0.887	0.179
	medium	1.134	0.368	1.019	0.053
	coarse	1.000	0.000	1.000	0.000

TABLE I

RESULTS FOR THE THICKNESS ESTIMATION ALGORITHMS (NORMALIZED).

of the mid-plane mesh (see equation 1), gives a fast hint of whether or not the estimation process is converging towards the correct value. It is a global metric, however, thus it does not capture whether there are local errors on the estimates that can be smoothed away by the averaging process. Furthermore, it would not convey useful information if the real thickness varied from element to element.

$$\bar{T} = \frac{1}{N} \sum_{i=1}^N \tilde{T}_i \tag{1}$$

**Root Mean Square Error (RMSE)** - RMSE takes the square of the individual differences, also called residuals, between the estimated and the real thickness at each element of the mid-plane mesh and aggregates them onto a single metric that has predictive power and is perceived as a good measure of accuracy [24] (equation 2). The lower the RMSE the better the thickness estimates produced by the associated algorithm. RMSE heavily weights outliers (i.e., particularly bad local estimates) due to the squaring of the residuals, whereas small residuals are attributed very small weights; it is felt, however, that for Finite Element Analysis of structural properties outliers can strongly affect the simulation result, thus this is a desirable property.

$$RMSE = \sqrt{\frac{\sum_{i=1}^N (\tilde{T}_i - T_i)^2}{N}} \tag{2}$$

**B. Results Analysis**

Results for the 7 synthetic parts, with 3 different mid-plane mesh resolutions and for two thickness estimation algorithms, are presented in table I.

In those cases where the midplane mesh runs outside the part's surface (parts 1 to 4) both algorithms fail to find valid

points on both sides of the mesh and, consequently, fail to estimate the thickness. Figures 4(a) and 4(b) illustrate this for Part 3.

The hole prevents the algorithms from finding valid points on the part's surface. The particular values presented at table I for parts 1 to 4 result from the fact that an estimate  $\tilde{T}_i$  equal to zero was generated for these cases; this is particularly evident for Part 1 where estimates could not be generated for any element since all of them are outside the part, thus resulting on  $\bar{T} = 0.0$ . The fact that the midplane mesh is outside the part's surface means that it is not a good representation of the original part; these situations will be handled explicitly (see section III).

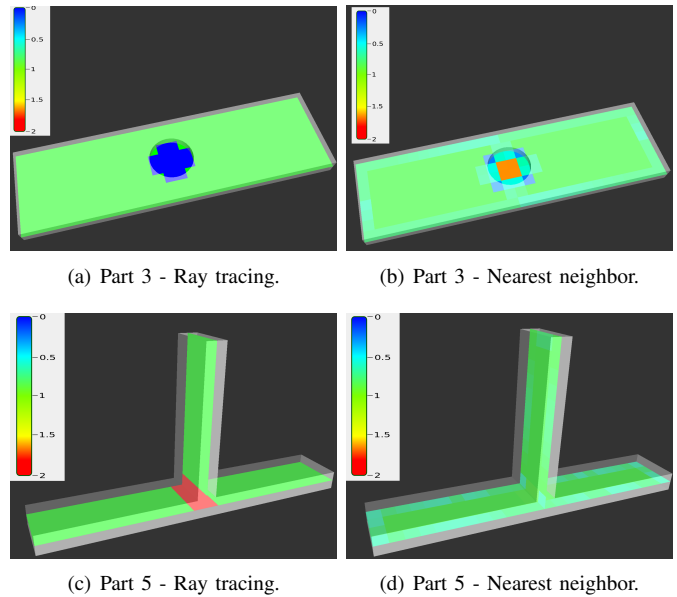


Fig. 4. Thickness estimation within holes and near ribs - pseudo color maps (normalized).

Parts 5 to 7 illustrate situations where ribs are present. It is evident that the ray tracing approach fails when the midplane mesh element's centroid is aligned with the rib - rays, which are shot along the element's normal, will run inside the part, finding an intersection at distant points of the part's surface and overestimating thickness (figure 5(a)). This is particularly evident for the finer granularity meshes. The NN algorithm does not suffer from this problem. It will still be able to find nearest points near the rib's junction with the part's surface, thus avoiding large thickness estimation errors (figure 5(b)). Figures 4(c) and 4(d) clearly show that the NN algorithm outperforms RT at these particular regions.

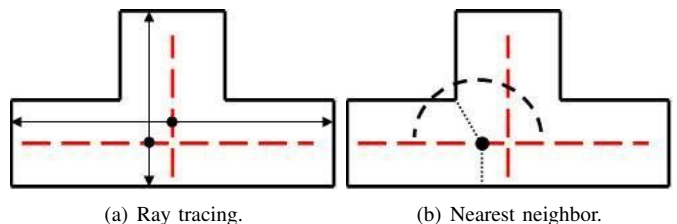


Fig. 5. Thickness estimation near ribs. Black lines represent the part's geometry, whereas the red dashed line represents the midplane mesh.

Table I also shows a somehow surprising result: the error of the NN algorithm tends to increase as the mesh granularity becomes thinner. Figures 4(b) and 4(d) illustrate why. When searching for the nearest point in the part's surface, the elements that are close to the mesh boundaries find the part's lateral surface as its closest neighbor (see figure 6). The thickness estimate is thus smoothed and will diverge from its actual value, suggesting a round edge. A solution for this divergence, which occurs with most parts, is discussed in section III.

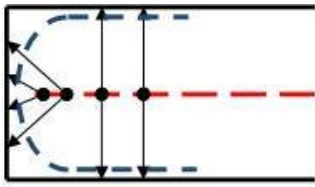


Fig. 6. Divergence of the NN algorithm close to the midplane mesh boundaries.

Summarizing, both algorithms produce wrong thickness estimates when the mid-plane mesh is a very inaccurate approximation of the part's geometry and runs outside it - a technique will have to be developed to handle these cases explicitly. Additionally, the ray tracing algorithm overestimates thickness in the presence of ribs, whereas the nearest neighbor algorithm underestimates thickness near the midplane mesh boundaries.

### III. ESTIMATION IMPROVEMENT

#### A. Inaccurate midplane meshes

The coarser the granularity of the mid-plane mesh the worst its accuracy as an approximation of the part's geometry. Often, this results on the mid-plane mesh running outside the part's surface, which leads to thickness estimation errors, as shown in the previous section. Two different cases occur with this inaccurate representation of the part's geometry: either the mesh is outside the surface but it still encompasses the part's geometry (parts 1 and 2, figures 3(a) and 3(c)), or the mesh runs outside the surface but this does not correspond to any region of the part's geometry (parts 3 and 4, figures 3(d) and 3(e)).

Detecting whether an element's centroid is contained within the part's volume is a generalization of the well-known point in polygon problem and can be solved by resorting to ray tracing: if a ray is shot from a given point along any direction, that point is inside the closed surface if it intersects the surface an odd number of times, else it is outside the closed surface [25]. Thus, for each centroid, one ray is shot along the element's normal direction for each side of the element. If each of these rays intersects the surface an odd number of times, then the centroid is inside the part. If both rays intersect the surface an even number of times, then the centroid is outside the surface. In this latter case, and if at least one of the rays intersects the surface more than zero times, the side of the centroid whose ray reported the closest intersection is selected as the one closest to the surface and thickness is estimated as

the difference between the two closest intersections of that ray. This process is depicted in figure 7. The part's surface is represented by the solid black lines, the mid-plane mesh is depicted by the dashed red line and the rays correspond to the blue arrows. The brackets represent the estimated thicknesses by subtracting the distances found by the two closest intersections along the same ray.

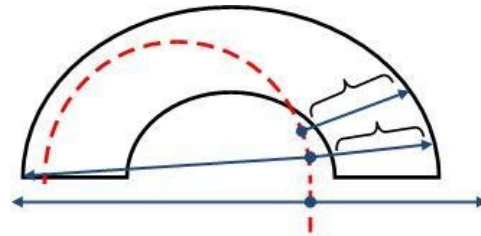


Fig. 7. Detection of whether the midplane mesh is outside the part's surface.

Parts 1 and 2 illustrate two cases where the mid-plane mesh is outside the part's surface but still encompasses it. By detecting whether each element's centroid is outside the part the exact thickness is found and a RMSE equal to zero is obtained (figure 8).

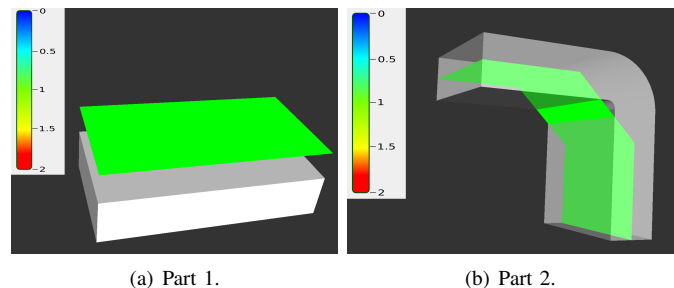


Fig. 8. Parts 1 and 2 with RT corrected thickness estimation - pseudo color.

The effectiveness of the RT corrected thickness estimation is also shown with a real part representing a B-pillar trim where a significant number of elements of the midplane elements are outside the part's surface, as illustrated in figure 9. Figure 10 shows thickness estimations obtained with RT and NN (left and center) and with the detection of elements outside the part's surface (right).

However, for some elements of the mid-plane mesh no intersections are found on either side of the element, as illustrated in the bottom part of figure 7. This happens within the hole of part 3 and on part 4 on the region of the mesh that extends further than the part's surface. Such elements are tagged as "Incorrect" and can later be post-processed (either manually or through other automated procedures under development).

#### B. Nearest neighbor divergence

In order to limit the divergence occurring near the midplane mesh boundaries with the NN algorithm, a limitation has been imposed on the maximum acceptable angle between the element's normal and the direction defined by the element's centroid and the surface nearest point. By limiting this angle it

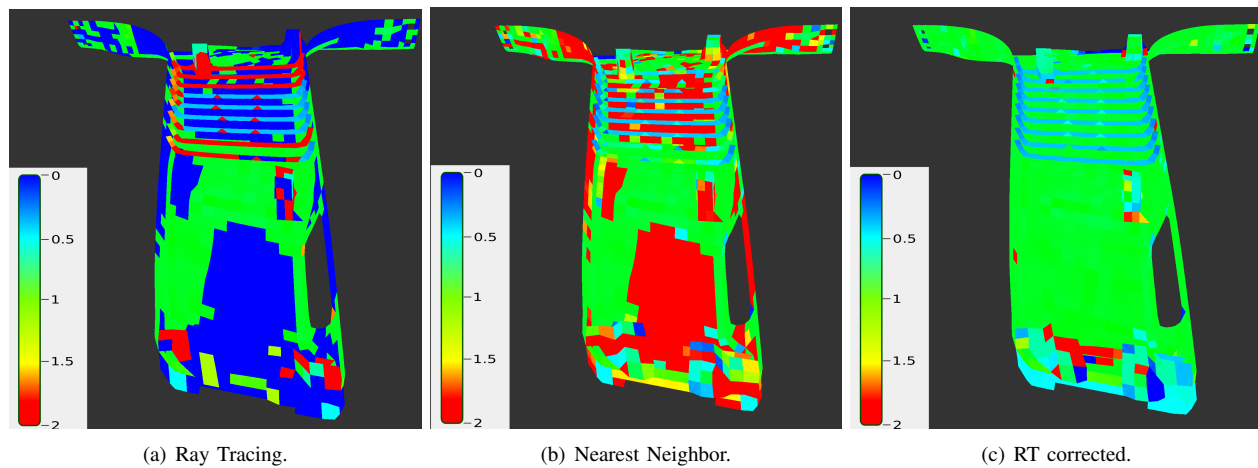


Fig. 10. Thickness estimation for the door pillar - pseudo color (normalized).

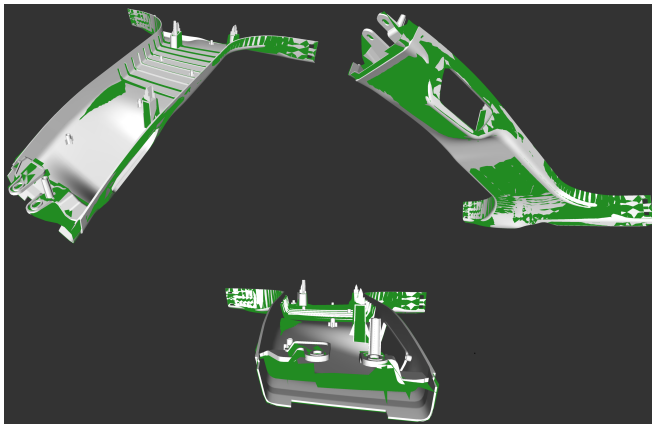


Fig. 9. Door pillar geometry and mesh: green and yellow correspond to midplane elements outside the part's geometry.

is expected that the part's lateral surface is rejected as a nearest neighbor, thus forcing the algorithm to expand its search onto regions of the surface that are farther away from the mid-plane element (Figure 11).

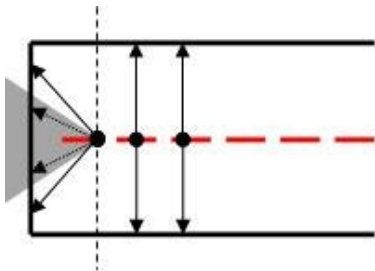


Fig. 11. Limiting acceptable angle for NN: the gray triangle represents the unacceptable angle domain, dashed arrows represent rejected nearest point directions, solid arrows represent accepted directions.

This technique requires some precaution. Some real part's geometries are modeled with polygons that have an area orders of magnitude larger than the respective midplane elements area. If the limitation of the angle is too strict, then some midplane elements could reject the surface polygon, missing

the correct nearest neighbor and overestimating local thickness. In the presence of ribs the angle rejection technique might also reject the correct nearest neighbor, resulting in overestimating thickness. The occurrence of these two cases depends on the geometric configuration of the part's surface and on the threshold applied to the angle. To study the impact of this technique different angle thresholds have been tested: 80, 65 and 45 degrees.

	Part 2	Part 5	Part 6	Part 7
RT	0.0008	3.0619	4.3301	0.3118
NN (no limit)	0.1688	0.1618	0.1414	0.1792
NN (80°)	0.0860	0.0741	0.0704	0.0848
NN (65°)	0.0273	0.0461	0.0447	0.0577
NN (45°)	0.0065	0.0118	0.0163	0.0493

TABLE II  
RMSE RESULTS FOR NN ANGLE LIMITATION WITH FINE MIDPLANE MESHES.

Table II presents the RMSE obtained for 4 different parts and respective fine grained midplane meshes. For these synthetic parts a threshold of 45° produces the smaller RMSE. However, for complex real parts such a large threshold results in many rejections and, consequently, in many local errors (see figure 12, where significantly wrong thickness estimates are highlighted in red). A threshold of 80° does not induce such errors and still its impact on the RMSE is significant more than halving it.

#### IV. CONCLUSION

This paper presents and analyzes two techniques, based on ray tracing (RT) and 3D nearest neighbor range search (NN) algorithms, to estimate local thicknesses from geometric models of automotive parts. These estimates are fundamental to allow accurate simulation of automotive part performance (e.g. deformation and fracture behavior) in high dynamic crash loadings by using finite element analysis (FEM). Results obtained using each of the algorithms individually (table I) allowed the identification of three different situations that lead to poor thickness estimation as measured by Root Mean Squared Error (RMSE): the midplane mesh runs outside the

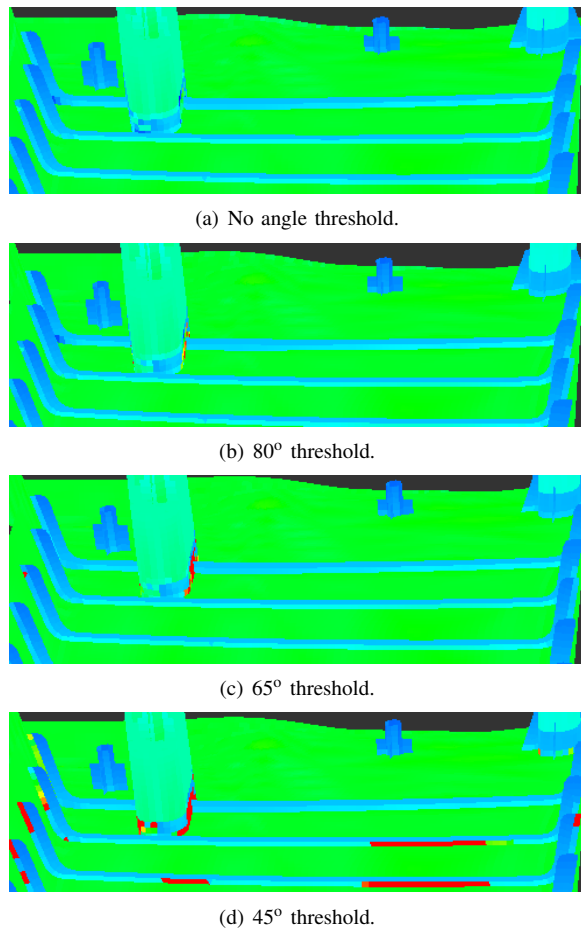


Fig. 12. Wrong thickness estimates (normalized) induced by limiting the maximum acceptable NN angle (highlighted in red).

part's surface preventing the proposed algorithms to find valid points on the part's surface, the NN algorithm diverges on the midplane boundaries and the RT algorithm fails to find accurate thicknesses on ribs.

The first problem was addressed by using ray tracing to detect whether an element's centroid is outside the surface. In such cases the difference between the two closest intersections detected on the same side of the element is used as thickness estimation. There are still some elements where no intersections are found on either side: these are tagged as as "Incorrect" for manual post-processing. The divergence with the NN algorithm near the midplane mesh boundaries was minimized by limiting the maximum angle allowed between the element's normal and the direction defined by the element's centroid and the nearest point on the part's surface. By requiring that this angle is less than a specific value RMSE was significantly reduced while avoiding other geometric errors. The ribs inaccuracies associated with the RT algorithm were not addressed explicitly since these are completely avoided by the NN algorithm.

The above results suggest that:

- NN fails on the midplane mesh boundaries but RT provides good estimates at these locations. The heuristic of limiting the angle reduces RMSE, but does not allow

estimates as good as RT; this is corroborated by the results achieved with part 2 (table II);

- RT fails on ribs, but NN provides good estimates at these locations.

Both algorithms complement each other: if each algorithm's best estimate can be selected for each element of the midplane mesh then RMSE is reduced. Figure 13 illustrates this approach for part 5: for each midplane element the estimate that minimizes the difference to the correct thickness was manually selected from the RT and NN with angle limitation algorithms. The final result is a very good overall estimate of the part's thickness, with an average mean of 1.0091 and RMSE equal to 0.0325. Small errors are visible only on the mid plane mesh boundaries on the rib joint with the part's main body, since these are the locations where both algorithms induce some inaccuracy.

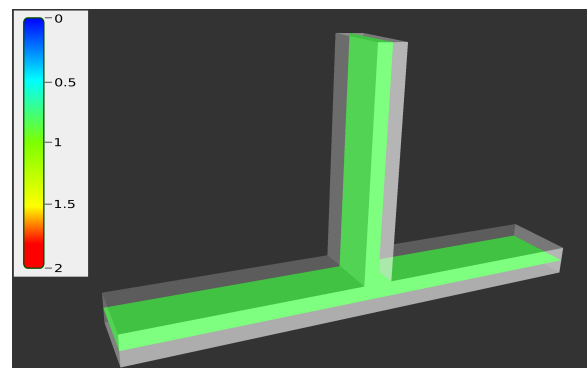


Fig. 13. Best estimate from either RT or NN manually selected for each midplane mesh element - pseudo color.

#### A. Future work

The above conclusion suggests that if a criterion can be found that allows automatic selection of either the RT or the NN estimate for each element, then RMSE can be significantly reduced and the whole results would be much more reliable from the FEM simulation process point of view. Such a criterion is not evident however, due to the complexity of real world parts. Real geometries and midplane meshes have lots of details and particular configurations that make it very difficult to establish which is the best estimate - particularly, the real local thicknesses are not known, since this is exactly the quantity that is being measured. Analysis of the local geometries in order to identify ribs and/or midplane mesh boundaries may also reveal too complex to be performed accurately.

A promising approach is to estimate thicknesses using both algorithms and then assign each estimate a given confidence weight given their relative variations within a given neighborhood. Identifying neighborhoods requires representing connectivity among midplane mesh elements; with this information some particular geometric arrangements, such as elements on the boundaries of the midplane mesh, can be identified, which will further facilitate the estimation of confidence weights. The final result would be a linear combination of both thickness estimates, weighted by the confidence values.

Future work will entail studying such alternative criteria, which will allow integrating the two algorithms presented throughout this paper. Once that criterion is established, the developed approach will be validated in two stages. First, it will be used to compare simulation results performed with the standard industry method of assigning the best-estimate overall thickness to the part, and those obtained by considering the local thickness distribution (for each individual midplane mesh element). Afterwards, results from simulations performed with best-estimate overall part thickness (traditional approach) will be compared to those from simulations taking into account the calculated local thickness (proposed approach), to verify which predicts most accurately the experimental tests.

## ACKNOWLEDGMENT

We acknowledge the Foundation for Science and Technology, Lisbon, Portugal, through the 3<sup>o</sup> Quadro Comunitário de Apoio and also the POCTI and FEDER programs.

## REFERENCES

- [1] T.Y. Yang, *Finite Element Structural Analysis*, Prentice-Hall (Englewood Cliffs, N.J.), ISBN 0133171167, 1986
- [2] R. Leithner, H. Zindler, A. Hauschke, Optimization of the Finite Volume Method Source Code by using Polymorphism, *International Journal of Mathematics and Computers in Simulation*, 1(3), pp. 228, ISSN: 1998-0159, 2007
- [3] S. Sabbagh-Yazdi, M. Alkhamis, M. Esmaili, N. Mastorakis, Finite Volume Analysis of Two-Dimensional Strain in a Thick Pipe with Internal Fluid Pressure, *International Journal of Mathematical Models and Methods in Applied Sciences*, 2(2), pp. 162, ISSN: 1998-0140, 2008
- [4] S. Sabbagh-Yazdi, N. Mastorakis, M. Esmaili, Explicit 2D Matrix Free Galerkin Finite Volume Solution of Plane Strain Structural problems on Triangular Meshes, *International Journal of Mathematics and Computers in Simulation*, 1(2), pp. 1, ISSN: 1998-0159, 2008
- [5] P. Frey and P. George, *Mesh Generation: Application to Finite Elements*, Hermes Science, ISBN 978-1903398005, 2000
- [6] H. Edelsbrunner, *Geometry and Topology for Mesh Generation*, Cambridge University Press (Cambridge, UK), 2001
- [7] J. Thompson and Z. Warsi and C. Mastin, *Numerical Grid Generation: Foundations and Applications*, North Holland, Elsevier, 1985
- [8] Jr. William Weaver and J. M. Gere, *Matrix Analysis Of Framed Structures*, Springer-Verlag New York, 1966
- [9] G. Strang and G. Fix, *An Analysis of The Finite Element Method*, Prentice Hall (Englewood Cliffs, N.J.), 1973
- [10] M. Brinkmeier and U. Nackenhorst and S. Petersen and O. von Estorff, A numerical model for the simulation of tire rolling noise, *Journal of Sound and Vibration*, 309(1), pp. 20–39, 2008
- [11] R. Lohner, *Applied Computational Fluid Dynamics Techniques: An Introduction Based on Finite Element Methods*, John Wiley & Sons, 2nd edition, ISBN: 978-0-470-51907-3, 2008
- [12] A. Hawkins and J. T. Oden, *Toward a predictive model of tumor growth*, Institute for Computational Engineering and Sciences (ICES), The University of Texas at Austin, 2008
- [13] R. Simões, A. Brito, A. Cunha, *Integration of Flow Simulation and Solid Modelling Software for Aluminium Mould Optimization*, O Molde, 69, pp. 26, 2006
- [14] V. Laemlaksakul, Design of Laminated Bamboo Furniture using Finite Element Method, *International Journal of Mathematics and Computers in Simulation*, 2(3), pp. 274, ISSN: 1998-0159, 2008
- [15] M. ILiescu, E. Nutu, B. Comanescu, *Applied Finite Element Method Simulation in 2D Printing*, *International Journal of Mathematics and Computers in Simulation*, 2(4), pp. 305, ISSN: 1998-0159, 2008
- [16] *Concurrent Engineering: Automation, Tools, and Techniques*, Andrew Kusiak (ed), Wiley-Interscience, ISBN: 978-0-471-55492-9, 1992
- [17] J. R. Hartley, S.Okamoto, *Concurrent Engineering: Shortening Lead Times, Raising Quality, and Lowering Costs*, 1998
- [18] D. Carstêa, *Semiautomatic Generation of Database in Finite Element Methods*, *International Journal of Mathematical Models and Methods in Applied Sciences*, 1(2), pp. 76, ISSN: 1998-0140, 2007
- [19] B. Kirk and J. W. Peterson and R. H. Stogner and G. F. Carey, libMesh: A C++ Library for Parallel Adaptive Mesh Refinement/Coarsening Simulations, *Engineering with Computers*, 22(3), pp. 237-254, 2006
- [20] E. De Sturler and G. H. Paulino and S. Wang, *Topology optimization with adaptive mesh refinement*, 6th International Conference on Computation of Shell and Spatial Structures, Ithaca, New York, USA, 2008
- [21] A. Appel, Some techniques for machine rendering of solids, *AFIPS Conferences*, 32, pp. 37–45, 1968
- [22] T. Whitted, An Improved Illumination Model for Shaded Display, *Communications of the ACM*, 23(6), pp. 343-349, 1980
- [23] M. de Berg, *Computational Geometry: Algorithms and Applications*, ISBN 3540656200, Springer, 2008
- [24] M. H. DeGroot, *Probability and Statistics*, Addison-Wesley (Reading, Massachusetts), 1980
- [25] M. Vandewettering and E. Haines and E. John Kalenda and R. Parent and S. Uselton and "Zap" Andersson and B. Holloway, *Point in Polygon, One More Time.... Ray Tracing News*, 1990